Development of Ligament Tissue Biodegradable Devices: A Review

A.C. Vieira [1,#] , R.M. Guedes [2], A.T. Marques [2]

[1] *Composite Materials Unit, Institute of Mechanical Engineering and Industrial Management, avieira@inegi.up.pt*

[2] *Mechanical Engineering Department, Faculty of Engineering of Porto University, rmguedes@fe.up.pt; marques@fe.up.pt*

Abstract

This bibliographic review is focused on ligament tissue rehabilitation, its anatomy-physiology, and, mainly, on the dimensioning considerations of a composite material solution. The suture strength is problematic during the tissue recovering, implying reduction of mobility for several months. However, early postoperative active mobilization may enable a faster and more effective recovering of tissue biomechanical functions. As the risk of tendon rupture becomes a significant concern, a repair technique must be used to withstand the tensile forces generated by active mobilization. However, to avoid stress shielding effect on ligament tissue, an augmentation device must be designed on stiffness basis, that preferably will decrease. Absorbable biocomposite reinforcements have been used to allow early postoperative active mobilization and avoid the shortcomings of current repair solutions. Tensile strength decrease of the repair, during the initial inflammatory phase, is expected, derived from oedema and tendon degradation. In the fibroblastic phase, stiffness and strength will increase, which will stabilize during the remodelling phase.
The reinforcement should be able to carry the dynamic load due to locomotion with a mechanical behaviour similar to the undamaged natural tissue, during all rehabilitation process. Moreover, the degradation rate must also be compatible with the ligament tissue recovering. The selection and combination of different biodegradable materials, in order to make the biocomposite reinforcement functionally compatible to the damaged sutured tissue, in terms of mechanical properties and degradation rate, is a major step on the design process. Modelling techniques allow pre clinical evaluation of the reinforcement functional compatibility, and the optimization by comparison of different composite solutions in terms of biomechanical behaviour.

KEYWORDS: biodegradable polymers, aliphatic polyesters, hydrolytic degradation rate, dimensioning, healing process

[#] Corresponding author's contacts:
Campus FEUP, Rua Roberto Frias 400
4200-465 Porto, Portugal
Tel.:+ 351229578710; fax:+ 351229537352
E-mail address: aveira@inegi.up.pt

1. Introduction

Over 800,000 people seek medical care each year for injuries to ligaments and tendons (Butler et al., 2003). Ruptures or tearing can cause great pain and instability, impairing the functionality of the joint complex. There are numerous areas throughout the body where tendons and ligaments experience such injuries. The anterior cruciate ligament (ACL) is the most commonly injured ligament of the knee, with over 150,000 ACL surgeries performed annually in the United States (Cooper et al., 2004).

It is common to intraarticular ligaments to have a limited capacity to heal (Khatod et al., 2003; Louie et al., 1998), due to low vascularization. For these cases, the simple suture back together is an ineffective repair procedure. Hence, the use of grafts is often required in reconstruction surgery (Woo et al., 2006). Unfortunately, material selection and dimensioning have been problematic. Long-term rupture or excessive laxity, are the main mechanical causes of failure.

Traditionally, ligaments and tendons injuries have been treated with biological grafts (autografts or allografts) (Amiel et al., 1990). Both possess good initial mechanical strength and promote cell proliferation and incorporation of the graft on the new tissue formation. However, they suffer from a number of disadvantages. Although autograft is the current gold standard used in around 90% of the ACL reconstructions, inherently require additional surgery which has been known to cause donor site morbidity, increased recovery time, and possible pain at the harvesting site (Cartmell et al., 2004; Kim et al., 2003). Allografts are limited in supply with associated risks of disease transmission and immunogenic response from the host (Cameron et al., 2000; Cartmell et al., 2004; Kim et al., 2003; Vunjak-Novakovic et al., 2004). Alternatively, attempts have also been made to use synthetic materials in ligament replacements. Non-degradable synthetic materials that have been used for ACL repair include carbon fibers, polyethylene terephthalate (Leeds-Keio ligament), polypropylene (Kennedy Ligament Augmentation Device), and polytetrafluoroethylene (Gore-Tex) (Amiel et al., 1990; Arnoczky, 1983; Silver et al., 1991; Smith et al., 1993; Snook, 1983). These synthetic devices fail due to stress shielding of new tissue formed, long-term rupture by fatigue, excessive laxity due to material creep, or to fragmentation and wear debris (Noyes and Grood, 1976; Ward, 1983), problems which can eventually lead to other associated joint problems. Some of these synthetic ligament replacements have been conditionally approved by the FDA only for revision surgeries (McPherson et al., 1985).

Excessive laxity is a progressive failure process that, in some cases, can be self-repaired by the adaptation and compensation of the other tissues involved in the articular complex. Long-term rupture by fatigue is a more dangerous failure cause, since the sudden failure may damage the surrounding tissues.

The current described shortcomings of biological and synthetic grafts in repair of tendons and ligaments may be overcome through the use of biodegradable materials. A successful biodegradable graft must be biocompatible, display similar mechanical behavior when swelled to saturation (shape of the stress–strain and stress relaxation response), have endurance strength (fatigue resistance at the same frequency of the application), be creep resistant, degrade at a rate that does not cause stress shielding or rupture of the new tissue, and promote tissue ingrowth.

One method to validate the functional compatibility is to compare the properties of the graft to those of the natural tissue, using the same biomechanical parameters such as the dynamic forces, strains and frequencies that are present during medium aggressive daily functions, and along the rehabilitation. In the design process, damage modeling, either by degradation or fatigue/creep, is a helpful tool in predicting outcomes and to analyze and optimize functional compatibility, previously to *in vivo* validation.

2. Constituents of ligament tissues - Function and structure

Tendons and ligaments are dense, regularly arranged, connective tissues that induce or guide joint movement, working as elastic energy absorbers. Tendons attach muscle to bone and are what couples the force of a muscle to a movement in the skeletal structure (Martin et al., 1998). Ligaments attach bone to bone in order to limit the movement of bones with respect to each other (Martin et al., 1998). Both are passive tissues working as springs mainly under tension, and therefore they have

similar structural characteristics (Martin et al., 1998; Wang, 2006).

The overall tissue structure (see Figure 1) consists mainly of fibroblasts surrounded by collagen fibrils along with small amounts of proteoglycans (Martin et al., 1998; Khatod and Amiel, 2003). While the fibroblasts themselves do not comprise a large volume of tendon/ligament tissue, they are responsible for secreting and remodeling the ECM (extra cellular matrix). However, the relatively low numbers of fibroblasts, along with their low mitotic activity, lead to a relatively low tissue turnover rate and may explain why some tendons and ligaments seem to possess a poor capacity for natural healing (Louie et al., 1998). ECM contains a hierarchical structure with increasing levels of organization including collagen molecules, fibrils, fibril bundles, and fascicles. These structures are aligned parallel to each other along the long axis of the tissue and the direction of principle force, conferring, this way, highly anisotropic properties. The sinusoidal wave-like structure of the collagen fascicles, known as the ‘‘crimp’’ structure, explains the typical non linear behavior.

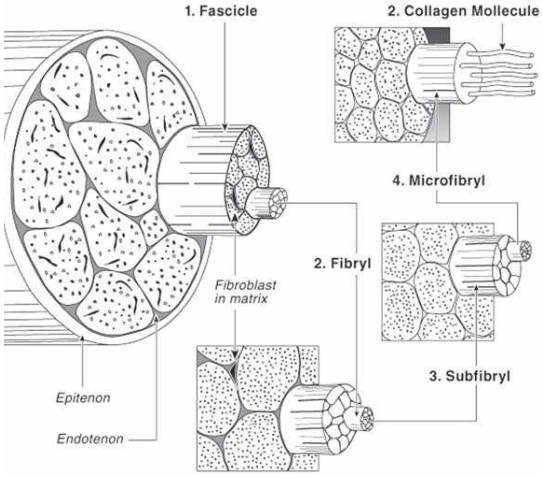

Figure 1 – Tendon structure (Wise et al., 1995a)

While all tendons and ligaments have these basic structural components, their mechanical properties can vary between different tendons and ligament tissues. For the same tissue, it can vary between individuals, and for the same tissue in the same individual may vary according to harvesting zone, depending upon their biomechanical function. However, they display, typically, 3 similar stages of behavior when tensile loaded. First there is an area where the ligament exhibits a low stiffness region known as the toe region. When a force is applied to the tissue, it is transferred to the collagen fibrils, resulting in lateral contraction of fibrils and the straightening of the crimp pattern. Following this, it displays an increase in stiffness, corresponding to the linear region. Since the collagen fibers are straightened, this corresponds to collagen stiffness. The yield and failure region is the last area. It exhibits a decrease in slope and represents the defibrillation of the ligament (Silver et al., 1991).

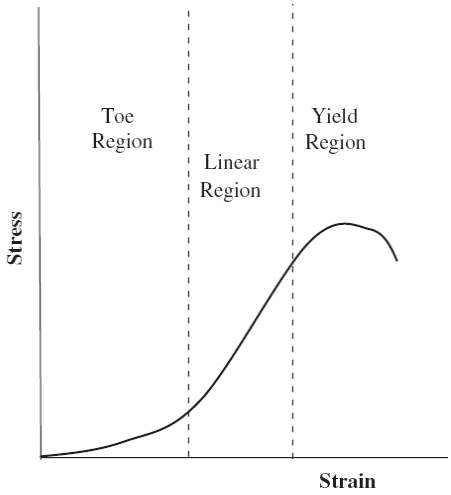

Figure 2 - Stress–strain behavior of ligament. (Freeman et al., 2006)

Collagen, mainly type I and III, is the largest component of the ECM for tendon and ligament tissue (Martin et al., 1998; Khatod and Amiel, 2003; Thomopoulos et al., 2003). In the case of ACL, the ratio of collagen I to collagen III is about 9:1 (Altman et al., 2002). The tensile strength is closely related to the presence of type I collagen produced by the fibroblast (Heller et al., 2006; Williams et al., 1984; Williams et al., 1980). Highly hydrated proteoglycans are distributed along ECM to facilitate lubrication between fascicles and its sliding (Vogel, 2004).

In table 1, the properties of human ACL are summarized up. According to Lui et al. (1997), the significant differences between male and female are due to estrogen decreasing the production of collagen (around 40%). Differences on mechanical properties among several references also depend upon the applied strain rate. It has been estimated that injuries occur at strain rates that range between 50%/s and 150,000%/s (Crowninshield and Pope,

1976). According to Pioletti et al. (1999), the stiffness of ACL is around 117N/mm (at 40%/s strain rate). Furthermore, the age has an effect on the decrease of linear stiffness, ultimate load and energy absorbed (Woo et al., 1991).

Table 1 - Properties of the Human ACL.

PROPERTIES OF THE HUMAN ACL		
Properties	**Values**	**Ref**
Length (mm)	**27 – 32** **31 – 38**	Freeman et al., 2006 Karmani and Ember, 2003
Toe Regions (strain)	**2.0% - 4.8%** **1.5% - 4.0%**	Chen and Black, 1980 Karmani and Ember, 2003
Tearing and Ligament Damage (strain)	**7% to 16%** **10% to 15%**	Chen and Black, 1980 Karmani and Ember, 2003
Human Physical Activity (N)	**67 – 700**	Chen and Black, 1980
Elongation at Failure (mm)	*Male:* **6.8 – 11** *Female:* **4.9 – 10**	Chandrashekar et al., 2006
Strain at Failure	*Male:* **24% - 36%** *Female:* **19% - 35%**	Chandrashekar et al., 2006
Load at Failure (N)	*Male:* **1119 – 2517** *Female:* **739 – 1793** **1725 – 2195** **2000 – 2300**	Chandrashekar et al., 2006 Karmani and Ember, 2003 Woo et al., 1991
Stress at Failure (MPa)	*Male:* **16.3 – 36.4** *Female:* **13.7 – 31.5**	Chandrashekar et al., 2006
Stiffness (N/mm)	*Male:* **219 – 397** *Female:* **111 – 287** **210 – 270**	Chandrashekar et al., 2006 Woo et al., 1991
Modulus of Elasticity (MPa)	*Male:* **93 - 163** *Female:* **49 - 149**	Chandrashekar et al., 2006

3. Augmentation device – Materials, Architecture and Dimensioning

There are many biomechanical considerations that should be taken into account when designing tendon or ligament tissue devices. The repairing should ideally fulfill all requirements of the healthy ACL (see Table 1). The ACL withstands cyclic loads of approximately 300 N during 1 to 2 million cycles per year, and it is regularly exposed to tensile forces up to 630 N (for jogging) (Chen and Black, 1980).

The established standards for ACL grafts are 1730 N for the tensile strength, 182 N/mm for linear stiffness, and 12.8 N.m for energy absorbed at failure (Noyes and Grood, 1976; Woo and Adams, 1990). However, we believe that a range of load bearing capacities and stiffness should be available, mainly dependent on the patient gender than on body weight.

Early in the rehabilitation process, the synthetic graft should protect the new tissue from the forces developed by active mobilization, but allow gradual increase of exposure to loading. This will permit the tissue to develop more naturally in a more effective way. The graft stiffness should ideally decrease, to avoid stress shielding.

In the autograft ACL reconstruction, patients usually resume normal daily activities around 3 months after surgery, and typically return to sports activity after 6 months. Full recovery to pre-injury sports level can generally be achieved between 9 and 12 months following surgery (Chen et al., 2006). Hence, for a biodegradable ligament device, its tensile fatigue/creep rupture strength should be above the stress applied to the graft. The strength will gradually be reduced in the recovery, while the injured ligament restores its full bearing capacity.

Materials

Biodegradable polymers can be divided into two groups, synthetic polymers and natural polymers. Degradation products must not be harmful to the surrounding host tissue and they should not result in unresolved inflammation or other harmful biological responses.

The most popular and important biodegradable synthetic polymers are: aliphatic polyesters, such as polylactic acid (PLLA and PDLA), polyglycolic acid (PGA), polycaprolactone (PCL), polyhydoxyalkanoates (PHA's) and polyethylene oxide (PEO) among others. As other thermoplastic materials they can be processed into fibers. However, each of these has some shortcomings which restrict its applications, due to inappropriate stiffness or degradation rate. Blending techniques are an extremely promising

approach which can be used to tune the original properties of the polymers (Aslan et al., 2000). Aliphatic polyesters are a central class of biodegradable thermoplastic polymers, because hydrolytic and/or enzymatic chain cleavage of these materials leads to α-hydroxyacids which, in most cases, are ultimately metabolized by the host. Since the 1970s, FDA has approved its use for a variety of clinical applications, (Wise et al., 1995a; Cooper et al., 2000; Laurencin et al., 1998; Wise et al., 1995b), e.g. for surgical sutures (Bendix, 1998; Vert, 1989), internal bone fixation (Stähelin et al.,1997) and drug delivery systems (Edlund and Albertsson, 2002), because they present good biodegradability, biocompatibility, and reasonably good mechanical properties. They have also been investigated for use in tissue engineering and regenerative medicine.

For this particular application, materials with a slower degradation should be selected. For these reason, PLLA has been widely used in ligament devices. It degrades completely into lactic acid within a period of between 10 months and 4 years depending upon its molecular weight, crystallinity, shape, and implantation site (Chen et al., 2003).

PCL presents a slower degradation than that of PLLA (Chen et al., 2003). Due to PCL low stiffness, it is commonly combined with PLLA to decrease its brittle behavior in slow degrading devices. These hydrophobic materials are less prone to swell, comparing to PGA or PEO. However, a lower wettability adversely affects cell adhesion.

The degradation rate of biodegradable polymers and their mechanical properties are also strongly influenced by their morphology and crystallinity. Generally, the biodegradation occurs first in the regions with lower crystallinity. Independently of the degradation environment, there are numerous variables, such as the material's chemical structure, crystallinity, molecular weight, processing conditions, shape and size, affecting the polymer degradation mechanisms.

It is possible to control the hydrolytic rate constant of the material, and also its final mechanical properties, by block copolymerization or blending with other biodegradable polymers, having different characteristics. Another way to control the degradation rate and mechanical properties, in order to match the dimensioning requirements during all the healing process, is to use different yarns of fibers, composed of materials with different degradation rates. A wide range of degradation profiles and mechanical properties are possible using different fibers and varying diameter, architecture, and many commercially available materials (Altman et al., 2002; Freeman et al., 2006; Cooper et al., 2000; Laurencin et al., 1998).

Other biodegradable natural materials, like silk fibers were also proposed by Altman et. al (2002), mainly due to the very high strength, slow degradation and biocompatibility. These characteristics are due to the high homogeneity of the macromolecules, extensive hydrogen bonding, the hydrophobic nature of the protein, and the degree of crystallinity. Silk fibers lose the majority of their tensile strength only after 1 year *in vivo* (Altman et al., 2002). Silk comprises of a fibroin core and a sericin cover. Sericin causes adverse biocompatibility problems and hypersensitivity, and many processes have been used to remove it (Ma, 2008).

Collagen based constructions have also been used in ACL regeneration. Purified collagen derived from animals tissues must be processed to remove foreign antigen and potential disease transmission, improve its mechanical strength and to slow down the degradation rate by crosslinking. The unsuccessful application in ligament tissue engineering was due to relatively fast *in vivo* degradation and loss of mechanical strength (Liao et al., 2008).

Production Methods

Braiding is a technique that has been used to create products made of fibers designed to bear axial loads (Kawabata, 1989) and provide extension. Their design makes them shear resistant and conformable (Cooper, 2002). The simplest braids are composed of sets of yarns that follow circular paths in opposite directions with a sequence of crossovers that cause the yarns to interlace forming a fabric (Kawabata, 1989). The twisting of fibers can also be used to form yarns that can withstand the braiding process. Both the twisting direction and degree of twisting affect yarn strength, abrasion resistance, and flexibility (Hudson et al., 1993). Low twist produces weaker yarns that pull apart more easily (Hudson et al., 1993). As the amount of twist is increased the strength and level of abrasion resistance of the yarns

are increased. If the yarns are wound too tightly (and the fibers become more perpendicular to the long axis of the yarn) the strength and abrasion resistance decrease (Hudson et al., 1993). The scaffold composite architecture should be designed to accurately mimic the biomechanical profile and mechanical properties of the tissue (Freeman et al., 2006; Horan et al., 2006). In recent work of Laurencin et al. (2006), braid–twist scaffolds of PLLA fibers resulted in a significant increase in the ultimate tensile strength, an increase in ultimate strain, and an increase in the length of the toe region when compared to braided and twisted fiber scaffolds alone. Altman et al. (2002), studied the yarn design of silk fibers in terms of functional compatibility, and concluded that braiding alone has a limited change in stiffness following the locking-angle.

The architecture of the tissue-engineered scaffold is an important design consideration also because it can modulate biological response and long-term clinical success of the scaffold. It has been reported that calcified tissue ingrowth can occur at a minimum pore size of 100 μm (Spector et al., 1978). In addition, a minimum pore diameter of 150μm is suggested for bone and 200-250μm for soft tissue ingrowth (Konikoff et al., 1974) The presence of pore interconnectivity extending through an implant increases the overall surface area for cell attachment, which in turn can enhance the regenerative properties of the implant by allowing tissue ingrowth into the interior of the matrix (Freeman et al., 2006). The scaffolds can vary in terms of architecture (pore diameter, porosity, surface area), and mechanical properties (tensile modulus, maximum tensile load) under tensile testing, according to fabrication parameters such as materials selection, fibers diameter, braiding and twisting angles and yarn density (Cooper et al., 2004). As the braiding angle increases both the porosity and mode pore diameter significantly decrease, whereas the pore surface area significantly increases (Freeman et al., 2006). Hence, overall scaffold porosity can modulate the functionality and gross cellular response to the implant.

Biodegradable fibre-based scaffolds have been widely used for tendon and ligament tissue engineering and have proven to favour cellular proliferation and collagenous matrix deposition, which is crucial for tendon / ligament reconstruction (Li et al., 2002). Attempts to improve biocompatibility of the scaffolds using a gel system, such as fibrin or collagen gel for cell seeding, demonstrate instability in a dynamic environment such as the knee joint (Li et al., 2002) and problems in nutrient transmission (Sahoo et al., 2007). Modification techniques of coating with nanofibres or collagen were particularly effective in aiding cell attachment, growth and proliferation, ECM deposition and tissue regeneration. Electrospun polymeric nanofibres possess a high surface area to volume ratio (Sahoo et al., 2007). This will allow an increased cell adhesion (Li et al., 2002; Sahoo et al., 2007; Zong et al., 2003). Through the process of electrospinning, fibres with diameters ranging from less than 3 nm to over 1 μm can be constructed (Lee et al., 2005). According to Sahoo et al. (2007), when fibroblasts are seed onto electrospun scaffolds in which the nanofibres are longitudinally oriented, they take a spindle-shaped morphology and synthesize more collagen matrix than when they are seeded on a randomly oriented scaffold structure and subjected to uniaxial strain. This suggests that the morphology of the underlying scaffold may affect ECM production (Sahoo et al., 2007; Lee et al., 2005).

Design

The cord stiffness must be designed according to the stiffness of the natural ligament in its linear region, since the lower stiffness region (toe region) may be materialized by the twist and braiding architecture. One can use the law of mixtures to calculate the stiffness. The total load supported by the cord is equal to the sum of loads supported by each of the *n* fibres:

$$P_c = \sum_{i=1}^{n} P_i \qquad (1)$$

In tensile load $P_c = \sigma_c * A_c$ and medium stress, $\sigma_c * A_c = \sum_{i=1}^{n} \sigma_i * A_i$, where σ_i is the stress applied to each fibre and A_i is the cross section area of each fibre. The Voigth model is obtained for isostrain condition (Crawford, 1997):

$$\varepsilon_c = \varepsilon_1 = \varepsilon_2 = ... = \varepsilon_i = ... = \varepsilon_n \quad (2)$$

By dividing these two equations, and since Young modulus $E = \sigma / \varepsilon$:

$$E_c A_c = \sum_{i=1}^{n} E_n * A_n \quad (3)$$

Since the fibres have the same length, the cross-section area may be replaced by the respective volume fraction: $V_c=1$, V_1, V_2, …, V_i, …, V_n.

$$E_c = \sum_{i=1}^{n} E_n * V_n \quad (4)$$

Mechanical properties of polymeric materials, mainly thermoplastics, and also natural tissues, highly depend upon the strain rate applied to the specimen. As the strain rate increases, there is a transition from ductile to brittle behaviour. ACLs perform a load-unload cycle at 1.6 Hz (frequency), during fast walking, corresponding to a strain rate more or less 70%/s. Material tensile properties evolution during degradation must be determined at the same strain rate, on swollen specimens. The swelling has also a major significance on the visco-elastic properties of the material. When saturated, its ductile/brittle transition will occur at higher strain rates. This phenomenon is more significant for hydrophilic materials.

Laxity of ACL due to creep must not exceed 3-5 mm during all the rehabilitation. The muscles, the articular capsule and joint geometry work together and adapt, in some degree, to compensate ligament laxity and promote stability. However, excess laxity may result in knee instability and need of revision surgery (Chen et al., 2006).

Total load supported by the cord must be verified during designing, according to dynamic load requirements, to be under its fatigue strength for at least 500.000 cycles at 1,6Hz (fast walking during half year). Fatigue strength decrease, due to degradation, must be compatible to the regeneration of natural ligament.

4. Hydrolytic Degradation

The degradation process of biopolymers is composed of a sequence of reactions, mainly diffusion of aqueous solutions, and then hydrolysis mediated either by water and/or enzymes. The overall rate is determined by the slowest reaction, named the rate-limiting step. In the particular case of biodegradable polymers, water diffusion is very fast compared to water mediated hydrolysis. Simple hydrolysis is usually homogeneous, promoting bulk erosion. Since the large enzyme molecules can't diffuse, they promote surface erosion. Therefore, surface area, and porosity of the device are important factors to control the degradation rate when enzymatic degradation occurs (Cheung et al., 2007). In figure 3, the degradation mechanisms of an implanted biodegradable polymer are represented.

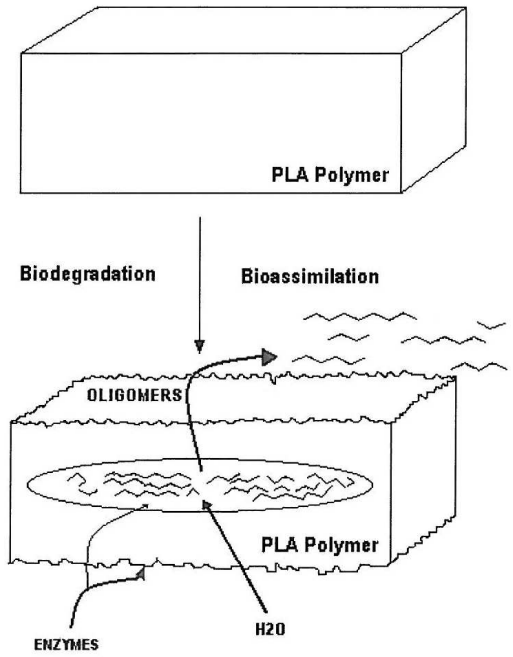

Figure 3 – Degradation mechanisms

In a biological environment, the degradation of polyesters is initiated by extracellular hydrolases, which are secreted by the micro-organisms to reduce the molar mass of the polymeric substrate (Tokiwa and Suzuki, 1977). Biodegradability of a certain polymer in the form of enzymatic hydrolysis is controlled by several factors. The most important is its chemical structure and the occurrence of specific bonds along its chains, like those in groups of esters, ethers, amides, etc., which might be susceptible to hydrolysis (Herzog et al., 2006; Nikolic et al., 2003; Noyes and Grood, 1976). For aliphatic polyesters, hydrolysis rates are affected by the temperature, molecular structure, ester group density as well as by the species of enzyme used. The degree of crystallinity may be a crucial

factor, since enzymes attack mainly the amorphous domains of a polymer (Marten et al., 2005).

Synthetic polymers, in contrast to natural polymers, are less susceptible to enzymatic hydrolysis, and so are generally degraded by simple hydrolysis. Their degradation rates have less variations from host to host, unless there are pH variations due to inflammations or implant degradation. Degradation products of PLA are known to reduce local pH, accelerate degradation and induce inflammatory reaction (Cheung et al., 2007). Blending it with PCL improves the local acidification, reducing the inflammatory response (Liao et al., 2008).

The degree of degradation is usually estimated from the mass loss or measuring the evolution of strength or the molecular weight (by size exclusion chromatography [SEC] or gel permeation chromatography [GPC]). The percentage of weight loss, ***WL%,*** was deduced from:

$$WL\% = 100(W_0 - W_r)/W_0 \qquad (5)$$

where W_0, and W_r, are the initial weight and the residual weight of the same carefully dried, partially degraded specimen, respectively.

Diffusion

The penetrating water rapidly creates a negative gradient of water concentrations from the surface to the centre, as expected from a pure diffusion viewpoint. However, this gradient vanishes in a couple of hours or days, depending on temperature and on material thickness and hydrophilicity. Since the diffusion of small molecules like water are rather fast, comparing with degradation rates, one can consider that hydrolysis of ester bonds starts homogeneously from the beginning. This is in agreement with the monomodal size exclusion chromatograms observed at the onset of molecular weight decreases (Li et al., 1990-2).

When a process is controlled by diffusion, the water concentration (W) is determined using Fick's equation, presented for 1D (Crank, 1975) in this case of isotropic polymers.

$$\frac{dW}{dt} = d\frac{\partial^2 W}{\partial x^2} \qquad (6)$$

The diffusion rate *d* can be determined by inverse parameterization, measuring the increase in weight due to moisture absorption during incubation, on samples with two different diameters. The amount of absorbed water is deduced from:

$$W = 100(W_s - W_r)/W_r \qquad (7)$$

where W_s, and W_r are the weight of the swollen specimen (after wiping the surface with paper) and the weight when dry, respectively.

Hydrolysis

The macromolecular skeleton of many polymers is comprised of ester groups. These groups can go through hydrolysis leading to chain scissions (see figure 4). A general consequence of such a process is the lowering of the plastic flow ability of the polymer, thus causing the change from ductile behavior into a brittle one or, if the behavior was initially brittle, an increase in the brittleness. Furthermore it is expected that brittleness also depends upon the strain rate and swelling. Moreover, after hydrolysis has started, brittleness may occur at lower strain rates.

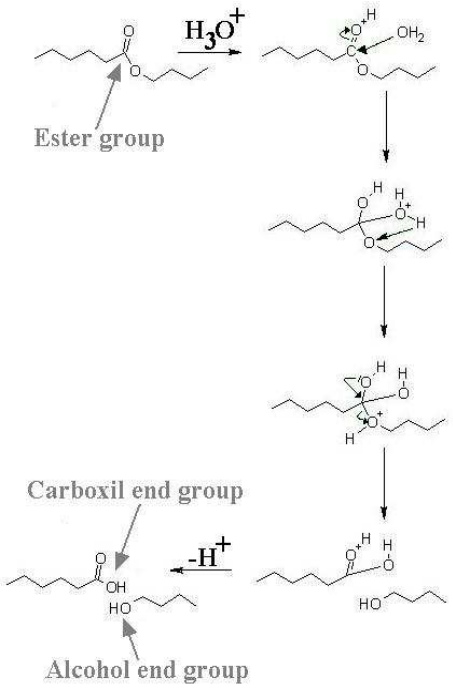

Figure 4 – Scheme of the most important hydrolysis mechanism

Hydrolysis has traditionally been modeled using a first order kinetics equation based on the kinetic mechanism of

hydrolysis, according to the Michaelis–Menten scheme (Bellenger et al., 1995). According to Farrar and Gillson (2002) the following first-order equation describes the hydrolytic process relative to the carboxyl end groups (C), ester concentration (E) and water concentration (W):

$$\frac{dC}{dt} = kEWC = u_m C \quad (8)$$

where u_m is the medium hydrolysis rate of the material , k is the hydrolysis rate constant E and W are constant in the early stages of the reaction. In addition, water is spread out uniformly in the sample volume (no diffusion control).

Using the molecular weight, and since the concentrations of carboxyl end groups are given by $C = 1/M_{n_t}$; the equation 8 becomes:

$$M_{n_t} = M_{n_0} e^{-u_m t} \quad (9)$$

where M_{n_t} and M_{n_0}, are the number-average molecular weight, at a given time t and initially at $t=0$, respectively.

Or using the scission number n_t per mass unit, as presented in (Bellenger, 1995), at time t is given, and the initial concentration of carboxyl end groups C_0 is known, the equation 8 becomes:

$$\frac{dn_t}{dt} = kEW(C_0 + n_t) \quad (10)$$

The experimental measurement of molecular weights allows the determination of n_t, and consequently the degradation rate constant:

$$n_t = \frac{1}{M_{n_t}} - \frac{1}{M_{n_0}} \quad (11)$$

These equations lead to a relationship $Mn = f(t)$. However, in the design phase of a biomedical device, it is important to predict the evolution of mechanical properties like tensile strength, instead of molecular weight. It has been shown (Ward, 1983) that the fracture strength of a generic thermoplastic polymer can, in many cases, be related to M_n through the relationship:

$$\sigma = \sigma_\infty - \frac{B}{M_{n_t}} = \sigma_\infty - \frac{B}{M_{n_0} e^{-u_m t}} \quad (12)$$

where σ is the fracture strength, σ_∞ is the fracture strength at infinite molecular weight, and B is a constant. As this is an empirical equation, the constant B must be determined for each material. One can thus determine the limit strength for the device that weakens during the recovering of the ligament, $\sigma_d = f(t)$, which must be above the maximum stress applied. The variation of the tensile strength along with degradation time is presented in figure 5, changing with initial molecular weight. According to Farrar and Gilson (2002) the rate constant k depends on the structure of the polymer, and is independent of its initial molecular weight.

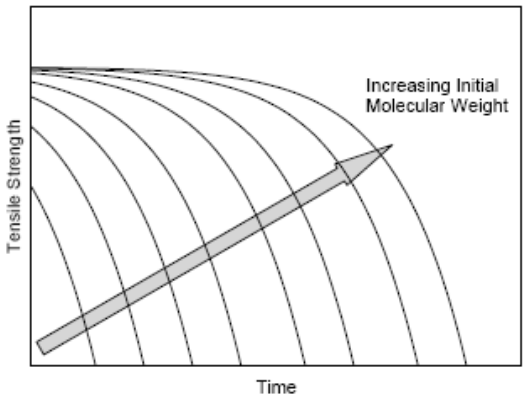

Figure 5 - Tensile strength vs time for different initial molecular weight (Farrar and Gilson, 2002)

In the case of a ligament tissue, the stiffness of the augmentation device should be compatible to the stiffness of the new formed tissue. However, stiffness does not depend upon M_n.

Critical Thickness and Hydrophilicity variation

We can define as (Bellenger, 1995) the characteristic time of hydrolysis, as the inverse of degradation ratio:

$$\tau_H = \frac{1}{u_m} \quad (13)$$

However, in order to allow the reaction medium to react with an ester group, it is necessary that it diffuses to this group. If L is the sample thickness, we can define a characteristic time of diffusion, τ_D:

$$\tau_D = \frac{L^2}{d} \quad (14)$$

We assume that the sample surface is large enough so that we can neglect the side effects.

According to Göpferich's opinion (1996), all degradable polymers could undergo surface erosion or bulk erosion at different conditions. The way a polymer matrix erodes depends upon the diffusivity of reaction medium inside the matrix, the degradation rate of the polymer's functional groups and the matrix dimensions.

When $\tau_H >> \tau_D$, the reaction medium reaches the core of the material before it reacts, and the degradation starts homogenously. This is called bulk erosion and is the case of water degradation of aliphatic polyester fibers. When $\tau_H << \tau_D$, the reaction medium reacts totally in the superficial layer and will never reach the core of the material. The degradation starts heterogeneously from the surface. Considering that diffusion rate of enzymes is zero, surface erosion is always the case of enzymatic degradation.

The critical thickness *Lc*, corresponding to $\tau_D=\tau_H$, is defined (Göpferich, 1996):

$$L_c = \sqrt{\frac{d}{u_m}} \quad (15)$$

Since diffusion and degradation rate both increase with temperature, however u_m increases more than *d*, hence the critical thickness will decrease with increasing temperature (Göpferich, 1996). It should be noted that if laboratory experiments are carried out on samples where the thickness is higher than the critical value, they will not necessarily model the case of fibers where the degradation mechanism due to water is bulk erosion. For semi-crystalline polymers the study becomes more complex, since only the amorphous phase is permeable to water.

Despite the homogenous beginning of hydrolytic degradation along the volume, for aliphatic polyesters it has been previously shown that it proceeds heterogeneously in the case of large size devices, the rate of degradation being greater inside than at the surface (Li et al., 1990-2; Grizzi et al., 1995; Li et al., 1990-1; Li et al., 1990-3; Vert et al., 1991). In this case, two phenomena are of critical importance. First, degradation causes an increase of the number of carboxylic chain ends which are known to autocatalyze hydrolysis, according to equation 8. Second, only oligomers which are soluble in the surrounding aqueous medium can escape from the matrix. As the degradation time increases, soluble oligomers which are close to the surface can leach out before total degradation, whereas those located well inside the matrix remain entrapped and contribute to the autocatalytic effect. This difference of concentration in acidic groups, results in the formation of a typical case of bulk erosion with the presence of hollows and a skin composed of less degraded polymer (Li et al., 1990-3).

The hydrophilicity involves the buildup of carboxyl end groups much more hydrophilic than the initial ester group (Van Krevelen, 1976). An increasing water equilibrium concentration with time can thus be expected. It is quite simple to solve the problem, as Bellenger et al. (1995) have shown, if we consider, with Van Krevelen (1976) that the water equilibrium concentration is an additive function, thus, $W = b + an$, and:

$$\frac{dC}{dt} = \frac{dn_t}{dt} = kE(C_0 + n_t)(b + an_t) \quad (16)$$

Solving this, after (Bellenger et al., 1995), leads to:

$$n_t = C_0 \left[\frac{b - aC_0}{be^{-kE(b-aC_0)t} - aC_0} - 1 \right] \quad (17)$$

Accordingly to Bellenger et al. (1995), for vinylesters, this approach gives a good account of the auto-accelerated character of the degradation due to the increase in water concentration. If the auto accelerated character is not due to increasing hydrophilicity, it is probably because its origin is in the hydrolysis mechanism and subsequent acidification. Hydroxyl groups coming from the first degradation steps can catalyze later hydrolysis reactions. Literature discussion is often contradictory.

5. Damage Modeling

The extent of distributed damage in a material can be characterized as Wang et al. (2003) done for polycarbonate, by a measurable macroscopic parameter, such as the residual fracture strain. Damage variable, including fatigue/creep and degradation, can be defined as:

$$D = \frac{\varepsilon_f - \tilde{\varepsilon}_f}{\varepsilon_f} = 1 - \frac{\tilde{\varepsilon}_f}{\varepsilon_f} \quad (18)$$

where ε_f is the fracture strain for a virgin sample, and $\tilde{\varepsilon}_f$ is the residual fracture strain after damage occurs by creep/fatigue and hydrolysis.

Damage is a time-dependent variable that can include fatigue and hydrolytic degradation. This simple analytical model allows the simulation of mechanical properties evolution during device degradation. However, this approximation considers separately damage due to fatigue and hydrolysis. Though, it is expected that these two mechanisms influence each other, since load will accelerate hydrolysis and hydrolytic damage will result in fatigue strength decrease.

Having determined the molecular weight and the mechanical properties at the n^{th} discrete time point, the damage equation due to hydrolysis and fatigue can be solved and it can proceed to the next time step. The resulting properties evolution must be compatible to natural tissue stiffness recovering.

Hydrolytic Damage

In order to perform computer simulations based on these models, the parameters degradation rate (u_m) and initial molecular weight (Mn_0) must be previously determined. Since the fibers are a thin element and diffusion occurs at about 37ºC, and considering that body fluids may flow rapidly inside the yarns, a degradation model for cords can be simplified assuming homogeneous hydrolyses. On that ground, the law of mixture may be used to determine the hydrolysis rate of the cord, considering homogeneous hydrolysis:

$$u_c = \sum_{i=1}^{n} u_m * V_n \quad (19)$$

In these conditions we defined damage due to hydrolysis as:

$$D_h = 1 - \frac{\sigma}{\sigma_0} = 1 - \frac{\sigma_\infty - \frac{B}{M_{n_t}}}{\sigma_\infty - \frac{B}{M_{n_0}}} \quad (20)$$

where σ_0 is the fracture strength for a virgin sample, and σ is the residual fracture strength after hydrolytic damage occurs.

Creep/Fatigue Damage

Continuum damage mechanics (CDM) are widely used for the determination of material failure under creep, fatigue and particularly creep–fatigue-interacted processes (Lemaitre and Chaboche, 1990). As the temperature increases, and minimum stress becomes significant the interaction between the processes of creep and fatigue can lead to significant reductions in product life. Unified constitutive models in terms of internal variables representing the damage caused by creep and fatigue, and the damage caused by their interaction, have thus been proposed (Tong and Vermeulen, 2003).

After a polymeric structure is subjected to a certain number of loading cycles, damage such as shear bands, micro-crazes, micro-cracks, macroscopic crazes and cracks may be formed. This damage can also reduce the material integrity, leading to a residual fracture strain that is lower than that for a perfect virgin structure.

The fatigue damage, D_f, evolution per cycle can be expressed as (Wang et al., 2003):

$$\frac{dD_f}{dN} = \left[\frac{\Delta\sigma^2}{2ES_0(1-D_f)^2}\right]^{s_0} \left[1-(1-D_f)^{1+2s_0}\right]^{\varepsilon_f} \quad (21)$$

where s_0 and S_0 are the material characteristic constants.

Assuming that the damage variable D_f is zero at the beginning of the cyclic loading, that is, when $N=0$, $D_f=0$. Then the damage value at any cycle, due exclusively to fatigue, can be determined by integrating Eq. (21),

$$\int_0^{D_f} \frac{d\left[1-(1-D_f)^{1+2s_0}\right]}{\left[1-(1-D_f)^{1+2s_0}\right]^{\varepsilon_f}} = \int_0^{N} (1+2s_0)\left(\frac{\Delta\sigma^2}{2ES_0}\right)^{s_0} dN \quad (22)$$

Thus, the relation between the damage variable D_f and the number of cycles N is:

$$\left[1-(1-D_f)^{1+2s_0}\right]^{1-\varepsilon_f} = (1-\varepsilon_f)(1+2s_0)\left(\frac{\Delta\sigma^2}{2ES_0}\right)^{s_0} N \tag{23}$$

The fatigue life N_f can be represented by:

$$N_f = \frac{(2ES_0)^{s_0}}{(1-\varepsilon_f)(1+2s_0)}\Delta\sigma^{-2s_0} \tag{24}$$

Eq. (24) can be readily used to predict the fatigue life, and this equation can also be expressed in the following form (Wang et al., 2003):

$$\log N_f = B + A\log\Delta\sigma \tag{25}$$

where

$$B = \log\frac{(2ES_0)^{s_0}}{(1-\varepsilon_f)(1+2s_0)} \text{ and } A = -2s_0 \tag{26}$$

Young's modulus E and fracture strain ε_f can be determined from material tests at the same strain rate of the application. The stress amplitude $\Delta\sigma$ versus fatigue life N_f curve can be obtained by fatigue tests for polymers, at the same frequency of the application. Thus coefficients A and B can be determined through this curve. Finally s_0 and S_0 can be calculated by Eq. (26). The fatigue damage evolution equation can be obtained as (Wang et al., 2003):

$$D_f = 1-\left[1-\left(\frac{N}{N_f}\right)^{\frac{1}{1-\varepsilon_f}}\right]^{\frac{1}{1+2s_0}} \tag{27}$$

6. Conclusions

The current strategies applied to ligament reconstruction are satisfactory. However, the goal of improving these procedures and eliminating its associated complications will always be a project demand. Engineered ligament tissues are promising solutions, requiring the development of a biocomposite structure that not only support physiologically loads, but also possess architectures able to orientate cell adhesion and ECM deposition. In the conception of a tissue-engineered augmentation device for ligaments, both functional and biological compatibility should be attended. In this review paper, a generic approach towards these biomechanical requirements is presented. This approach may obviate many of the shortcomings of current techniques, while allowing patients to promptly return to activity.

The material selection and design of a biodegradable structure, able to deform with the convalescent ligament, avoiding its stress shielding, capable to support dynamic tensile loads during rehabilitation exercises, without excessive laxity associated to material creep, and able to degrade being gradually substituted by natural tissue during the process, have a major influence on healing. The dimensioning method proposed here is an iterative process based on a damage model that includes fatigue and hydrolyses. This model may allow the simulation of the mechanical properties evolution during biodegradation. In future works the authors intend to carry out an experimental verification of this model.

7. Acknowledgements

The authors would like to thank the Portuguese Foundation for Science and Technology (FCT) for financial support under the grant PTDC/EMEPME/70155/2006.

8. References

Altman, G., Horan, R.L., Lu, H.H., Moreau, J., Martin, I., Richmond, J.C., et al., 2002. Silk matrix for tissue engineered anterior cruciate ligaments. Biomaterials 23, 4131–4141.

Amiel, D., Billings, E., Harwood, F.L., 1990. Collagenase activity in anterior cruciate ligament: protective role of the synovial sheath. Journal of Applied Physiology 69, 902–906.

Arnoczky, S.P., 1983. Anatomy of the Anterior Cruciate Ligament. Clinical Orthopaedics and Related Research 172, 19–25.

Aslan, S., Calandrelli, L., Laurienzo, P., Malinconico, M., Migliaresi, C., 2000. Poly(d,l-lactic acid) / poly(caprolactone) blend membranes: preparation and morphological characterization. J. Mater. Sci. 35, 1615–1622.

Bellenger, V., Ganem, M., Mortaigne, B., Verdu, J., 1995. Lifetime prediction in the hydrolytic ageing of polyesters. Polym. Degrad. and Stab. 49, 91-97.

Bendix, D., 1998. Chemical synthesis of polylactide and its copolymers for medical applications, Polym. Degrad. Stab. 59, 129–35.

Butler, D.L., Dressler, M.R., Awad, H.A., 2003. Functional tissue engineering: assessment of function in tendon and ligament repair. In: Guilak, F., Butler, D.L., Goldstein, S.A., Mooney, D.J. (Eds.), Functional tissue engineering. Springer, New York, pp. 211-268.

Cameron, M. L., Mizung, Y., Cosgarea, A.J., 2000. Diagnosing and managing anterior cruciate ligament injuries. Journal of Musculoskeletal Medicine 17, 47–53.

Cartmell, J.S., Dunn, M.G., 2004. Development of cell-seeded patellar tendon allografts for anterior cruciate ligament reconstruction. Tissue Engineering 10, 1065–1075.

Chandrashekar, N., Mansouri, H., Slauterbeck, J., Hashemi, J., 2006. Sex-based differences in the tensile properties of the human anterior cruciate ligament. J. Biomech. 39, 2943–2950.

Chen, C.C., Chueh, J.Y., Tseng, H., Huang, H.M., Lee, S.Y., 2003. Preparation and characterization of biodegradable PLA polymeric blends. Biomaterials 24, 1167–1173.

Chen, C.H., Chuang, T.Y., Wang, K.C., Chen, W.J., Shih, C.H., 2006. Arthroscopic anterior cruciate ligament reconstruction with quadriceps tendon autograft: clinical outcome in 4–7 years. Knee Surg Sports Traumatol Arthrosc 14, 1077–1085.

Chen, E.H., Black, J., 1980. Materials design analysis of the prosthetic anterior cruciate ligament. J. Biomed. Mater. Res. 14, 567– 586.

Cheung, H.Y., Lau, K.T., Lu, T.P., Hui, D., 2007. A critical review on polymer-based bio- engineered materials for scaffold development. Composites: Part B 38, 291-300.

Cooper, J., Lu, H., Ko, F.K., Freeman, J.W., Laurencin, C.T., 2005. Fiber-based tissue engineered scaffold for ligament replacement: design considerations and in vitro evaluation. Biomaterials 26, 1523–1532.

Cooper, J.A., 2002. Design, optimization and in vivo evaluation of a tissue-engineered anterior cruciate ligament replacement. PhD. thesis, Drexel University Press, Philadelphia.

Cooper, J.A., Lu, H., Ko, F.K., Freeman, J.W., Laurencin, C.T., 2004. Fiberbased tissue-engineered scaffold for ligament replacement: design considerations and in vitro evaluation. Biomaterials 26, 1523–1532.

Crank, J., 1975. The mathematics of diffusion. In: Park, G.S. (Eds), Polymer. Clarendon Press, Oxford.

Crawford, R.J., 1997. Mechanical Behaviour of Plastics. In: Q.s. University (Eds), Plastics Engineering. Pergamon Press, Belfast.

Crowninshield, R.D., Pope, M.H., 1976. The strength and failure characteristics of rat medial collateral ligaments. The Journal of Trauma 2, 99–105.

Edlund, U., Albertsson, A. C., 2002. Degradable Polymer Microspheres for Controlled Drug Delivery. Adv. Polym. Sci. 157, 67–112.

Farrar, D.F., Gilson, R.K., 2002. Hydrolytic degradation of polyglyconate B: the relationship between degradation time,strength and molecular weight. Biomaterials 23, 3905–3912.

Freeman, J.W., Woods, M.D., Laurencin, C.T., 2007. Tissue engineering of the anterior cruciate ligament using a braid–twist scaffold design. J. Biomech. 40(9), 2029-2036.

Göpferich, A., 1996. Mechanism of polymer degradation and erosion. Biomaterials, 23, 103-114.

Grizzi, I., Garreau, H., Li, S., Vert, M., 1995. Hydrolytic degradation of devices based on poly[DL-lactic acid) size-dependence. Biomaterial 16, 305-311.

Heller, J., B.R., Seeger, T., Weissenback, A., Tuchler, H., Resnik, D., 2006. MR-imaging of anterior tibiotalar impingement syndrome: agreement, sensitivity and specificity of MR-imaging and indirect MRarthography. Eur. J. Radiol. 58, 450–460.

Herzog, K., Muller, R.J., Deckwer, W.D., 2006. Mechanism and kinetics of the enzymatic hydrolysis of polyester nanoparticles by lipases. Polym. Degrad. Stab. 91, 2486–2498.

Horan, R.L., Collette, A.L., Lee, C., Antle, K., Chen, J., Altman, G.H., 2006. Yarn design for functional tissue engineering. J. Biomech. 39(12), 2232-2240.

Hudson, P., Clapp, A., Kness, D., 1993. In:Joseph's Introductory Textile Science (6 th eds) Harcourt Brace Jovanovich College, New York.

Karmani, S., Ember, T., 2003. The anterior cruciate ligament - I. Current Orthopedics 17, 369-377

Kawabata, S., 1989. Nonlinear mechanics of woven and knitted materials. In: Chou, T.W., Ko, F.K. (Eds)Textile Structural Composites,: Elsevier Science. New York, pp. 67–116.

Khatod, M., Amiel, D., 2003. Ligament biochemistry and physiology. In: Pedowitz, O.C.J., Akeson, R.A. (Eds), Daniel's knee injuries. Lippincott Williams and Wilkins, Philadelphia, pp. 31-42.

Kim, C.W., Pedowitz, R., 2003. Part A: graft choices and the biology of graft healing. In: Pedowitz, O.C.J., Akeson, R.A. (Eds), Daniel's knee injuries, Lippincott Williams and Wilkins, Philadelphia, pp. 435-491.

Konikoff, J.J., Billings, W., Nelson, L.J., Hunter, J.M., 1974. Development of a single stage active tendon prosthesis. I. Distal end attachment. J. Bone Jt. Surg. Am. 56, 848.

Laurencin, C.T., Ko, F.K., Borden, M.D., Cooper, J.A., Li, W.J., Attawia, M., 1998. Fiber based tissue engineered scaffolds for musculoskeletal applications, in vitro cellular response. In: Proceedings Biomedical materials: drug delivery, implants and tissue engineering: Symposium. Materials Research Society, Boston.

Lee, C.H., Shin, H.J., Cho, I.H., et al., 2005. Nanofiber alignment and direction of mechanical strain affect the ECM production of human ACL fibroblast. Biomaterials 26, 1261-1270.

Lemaitre, J., Chaboche, J.L., 1990 In: Mechanics of Solid Materials. Cambridge University Press, Cambridge, pp. 346-443.

Li, S., Garreau, H., Vert, M., 1990. Structure-property relationships in the case of the degradation of massive aliphatic poly(a-hydroxyacids) in aqueous media. Part 2: degradation of lactide/glycolide copolymers: PLA37.5GA25. and PLA75GA25. J Mater. Sci. Mater. Med. 1, 131-139.

Li, S., Garreau, H., Vert, M., 1990.Structure-property relationships in the case of the degradation of massive aliphatic poly(α-hydroxyacids) in aqueous media. Part 1: poly(DL-lactic acid). J. Mater. Sci. Mater. Med. 1, 123-130.

Li, S., Garreau, H., Vert, M., 1990. Structure-property relationships in the case of the degradation of massive aliphatic poly(α-hydroxyacids) in aqueous media. Part 3: influence of the morphology of poly(L-lactic acid). J Mater Sci, Mater Med 1, 198-206.

Li, W.J., Laurecin, C.T., Caterson, E.J., Tuan, R.S., Ko, F.K., 2002. Electrospun nanofibrous structure: a novel scaffold for tissue engineering. J. Biomed. Mater. Res. 60, 613–621.

Liao, S., Chan, C.K., Ramakrishna, S., 2008. Stems Cells and Biomimetic Materials Strategies for Tissue Engineering. Materials Science and Engineering C 28, 1189-1202

Liu, S.H., Al-Shaikh, R.A., Panossian, V., Finerman, G.A., Lane, J.M., 1997. Estrogen affects the cellular metabolism of the anterior cruciate ligament. A potential explanation for female athletic injury. Am. J. Sport Med. 25, 704-709.

Louie, L., Yannas, I., Spector, M., 1998. Tissue engineered tendon. In: Patrick Jr., C.W., Mikos, A.G., McIntire L.,(Eds), Frontiers in tissue engineering. Elsevier Science Ltd., New York, pp.412-442.

Ma, P.X., 2008. Biomimetic materials for tissue engineering. Advanced Drug Delivery Reviews 60, 184-198.

Marten, E., Müller, R.J., Deckwer, W.D., 2005. Studies on the enzymatic hydrolysis of polyesters - II. Aliphaticearomatic copolyesters. Poly.Degrad. Stab. 88, 371-381.

Martin, R.B., Burr, D.B., Sharkey, N.A., 1998. Mechanical properties of ligament and tendon. In: Skeletal tissue mechanics. Springer, New York, pp. 309-347.

McPherson, G.K., Mendenhall, H.V., Gibbons, D.F., Plenk, H., Rottmann, W., Sanford, J.B., Kennedy, J.C., Roth, J.H., 1985. Experimental mechanical and histologic evaluation of the Kennedy ligament augmentation device. Clinical Orthopaedics and Related Research 196, 186–195.

Nikolic, M.S., Poleti, D., Djonlagic, J., 2003. Synthesis and characterization of biodegradable poly(butylene succinate-co-butylene fumarate)s. J. Eur. Polym. J 39, 2183-192.

Noyes, F.R., Grood, E.S., 1976. The strength of the anterior cruciate ligament in humans and Rhesus monkeys. J. Bone Jt. Surg., A 58, 1074–1082.

Pioletti, D.P., Rakotomanana, L.R., Leyvraz, P.K., 1999. Strain rate effect on the mechanical behavior of the anterior cruciate ligament-bone complex. Medical Engineering and Physics 21, 95–100.

Sahoo, S., Cho-Hong, J.G., Siew-Lok, T., 2007. Development of hybrid polymer scaffolds for potential applications in ligament and tendon tissue engineering. Biomed. Mater. 2, 169–173.

Silver, F.H., Tria, A.J., Zawadsky, J.P., Dunn, M.G., 1991. Anterior cruciate ligament replacement: a review. Journal of Long-Term Effects of Medical Implants 1, 135–154.

Smith, B.A., Livesay, G.A., Woo, S.L., 1993. Biology and biomechanics of the anterior cruciate ligament. Clinics in Sports Medicine 12, 637–670.

Snook, G.A., 1983. A short history of the anterior cruciate ligament and the treatment of tears. Clinical Orthopaedics and Related Research 172, 11–13.

Spector, M., Michno, M.J., Smarook, W.H., Kwiatkowski, G.T., 1978. A high-modulus polymer for porous orthopedic implants: biomechanical compatibility of porous implants. J. Biomed. Mater. Res. 12, 665–677.

Stähelin, A., Weiler, A., Rüfenacht, H., Hoffmann, R., Geissmann, A., Feinstein, R., 1997. Clinical degradation and biocompatibility of different bioabsorbable interference screws: A report of six cases. Arthroscopy 13, 238–244.

Thomopoulos, S., Williams, G.R., Gimbel, J.A., Favata, M., Soslowsky, L.J., 2003. Variation of biomechanical, structural, and compositional properties along the tendon to bone insertion site. J. Orthop. Res. 21, 413–419.

Tokiwa, Y., Suzuki, T., 1977. Hydrolysis of polyesters by lipases. Nature 270, 76–78.

Tong, J., Vermeulen, B., 2003. The description of cyclic plasticity and viscoplasticity of waspaloy using unified constitutive equations. Int. J. Fatigue 25, 413-420.

Van Krevelen, D.W., 1976. In: Properties of Polymers. Elsevier, Amsterdam.

Vert, M., 1989. Bioresorbable polymers for temporary therapeutic applications. Angew Makromol Chem, 166/167, 155–168.

Vert, M., Li, S.M., Garreau, H., 1991. More about the degradation of LA/GA-derived matrices in aqueous media. J. Control. Rel. 16, 15-26.

Vogel, K., 2004. What happens when tendons bend and twist? J. Musculosklet.. Neuronal Interact. 4, 202–203.

Vunjak-Novakovic, G., Altman. G., Horan, R., Kaplan, D.L., 2004. Tissue engineering of ligaments. Annu. Rev. Biomed. Eng. 6, 131–156.

Wang, B., Lu, H., Tang, G., Chen, W., 2003. Strength of damaged polycarbonate after fatigue. Theoretical and Applied Fracture Mechanics 39, 163–168.

Wang, J., 2006. Mechanobiology of tendon. J. Biomech. 39, 1563–1582.

Ward, I., 1983. In: Mechanical properties of solid polymers. Wiley & Sons, Chichester.

Williams, I.F., Heaton, A., McCullagh, K.G., 1980. Cell morphology and collagen types in equine tendon scar. Res. Vet. Sci. 28(3), 302–310.

Williams, I.F., McCullagh, K.G., Silver, I.A., 1984. The distribution of types I and III collagen and fibronectin in the healing equine tendon. Connect. Tissue Res. 12, 211–227.

Wise, D.L., Trantolo, D.J., Altobelli, D.E., Yaszemski, M.J., Gresser, J.D., Schwartz, E.R., 1995. In: Encyclopedic handbook of biomaterials and bioengineering—Part A: materials. Marcel Dekker, New York.

Wise, D.L., Trantolo, D.J., Altobelli, D.E., Yaszemski, M.J., Gresser, J.D., Schwartz, E.R., 1995. Encyclopedic handbook of biomaterials and bioengineering—Part B: applications. Marcel Dekker, New York.

Woo, S.L., Abramowitch S.D., Kilger, R., Liang, R., 2006. Biomechanics of knee ligaments: injury, healing, and repair. J Biomech. 39, 1–20.

Woo, S.L.Y., Adams, D.J., 1990. The tensile properties of human anterior cruciate ligament (ACL) and ACL graft tissues. In: Daniel, D., Akeson, W., O'Connor, J., (Eds), Knee Ligaments: Structure, Function, Injury, and Repair. NewYork, pp. 279–289.

Woo, S.L.Y., Hollis, J.M., Adams, D.J., Lyon, R.M., Takai, S., 1991. Tensile properties of the human femur-anterior cruciate ligament-tibia complex. The effects of specimen age and orientation. Am. J. Sports Med. 19(3), 217—225.

Zong, X., Ran, S., Kim, K.S., Fang, D., Hsiao, B.S., Chu, B., 2003. Struture and morphology changes during in vitro degradation of electrospum poly(glycolide-co-lactide) nonofibers membrane. Biomacromolecules, 4(2), 416-423.